Inorganic Chemistry

ARTICLE

pubs.acs.org/IC

Tris-*cis*-tris-*trans*-dodeca[organo(dimethylorganosiloxy)]-cyclododecasiloxanes $\{RSi(O)[OSiMe_2R']\}_{12}$. Self-Ordering Features

Elena V. Matukhina,[†] Yulia A. Molodtsova,[‡] Yulia A. Pozdnyakova,[‡] Mikhail I. Buzin,[‡] Viktor G. Vasil'ev,[‡] Dimitris E. Katsoulis,[§] and Olga I. Shchegolikhina*[,‡]

[†]Department of Physics, Moscow State Pedagogical University, Malaya Pirogovskaya St. 1, Moscow 119882, Russia

[‡]Institute of Organoelement Compounds, Russian Academy of Sciences, Vavilova St. 28, Moscow 119991 Russia

[§]Dow Corning Corporation, Midland, Michigan 48686, United States

Supporting Information

ABSTRACT: The molecular order and thermotropic transitions of tris-*cis*-tris-*trans*-dodeca-[organo(dimethylorganosiloxy)]cyclododecasiloxanes $\{RSi(O)[OSiMe_2R']\}_{12}$ (R = Ph, R′ = Me, CH_2Cl, Vi; R = Me, Et, Vi, R′ = Me) have been investigated using differential scanning calorimetry, thermogravimetric analysis, and X-ray scattering. The cyclododecasiloxanes with phenyl side groups (R = Ph) can form mesomorphic structures within a very wide temperature range. Compounds with R = Me and Vi are liquids and exhibit microphase separation above their glass transition temperature because of the different nature and structure of the organic R and trimethylsiloxy $OSiMe_3$ side groups. When the side group R = Et, a mesomorphic structure is formed in a substantially more narrow temperature region than that for cycles containing phenyl groups. Thus, the type of side group R in organocyclododecasiloxanes determines their ability for self-ordering into mesomorphic structures and the thermal stability of the mesomorphic state.

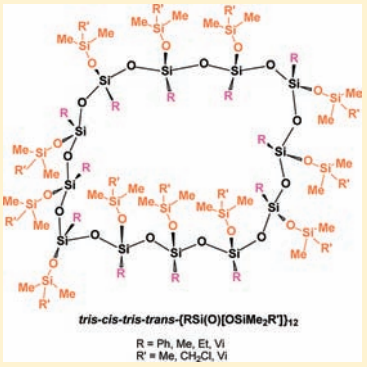

INTRODUCTION

Recently, we have shown[1−5] that organocyclosiloxanes (OCSs) are quite promising compounds, forming noncrystalline-ordered structures. This class of mesomorphic OCSs can be subdivided into four groups: two groups of cyclotetrasiloxanes with a general formula *all-cis*-$\{RSiO[OSiMe_2R']\}_4$ where R = Ph and R′ = Me, CH_2Cl, Vi[4] and also with R = Et, Pr^n and R′ = Me[3,4] (Figure 1a); a group of cyclohexasiloxanes *all-cis*-$\{RSiO[OSiMe_2R']\}_6$ with R = Ph and R′ = Me, CH_2Cl, Vi[2] (Figure 1b); the cyclopentasiloxane[5] *all-cis*-$\{PhSiO[OSiMe_3]\}_5$ (Figure 1c). With the exception of the pentamer, these cyclic organosiloxanes are crystallizable compounds and transform to a mesomorphic phase above the melting temperature of their crystalline phase. Cyclopentasiloxane is a noncrystallizable compound, but its molecules reveal a strong tendency to self-organize into ordered structures.[5]

Both the side group and the size of the siloxane ring influence the mesomorphic properties of the compounds. For the series *all-cis*-$\{PhSiO[OSiMe_3]\}_n$ (n = 4−6), the size of the siloxane cycle has no practical influence on the thermal stability of their mesomorphic state, as determined by the sublimation temperature. However, the cycle size affects the type of ordering of OCS molecules in the mesophase and the ability of OCSs to polymesomorphism.[1−5]

The nature of the substituent at silicon of cyclotetrasiloxanes *all-cis*-$\{RSiO[OSiMe_2R']\}_4$ and cyclohexasiloxanes *all-cis*-$\{RSiO[OSiMe_2R']\}_6$ influences the temperature range of the mesophase[1,2,4] but does not influence its structural organization.

The rather small size of the OCS cycles, investigated earlier, determines a compact form of their molecules that undoubtedly imposes certain restrictions on the possible variations of their self-organization in mesomorphic structures. Thus, we felt it was important to investigate the possibility of mesophase formation for OCS molecules of increased cycle size and, hence, its flexibility.

Cyclic organosiloxane compounds were prepared by a metal-ion-directed self-assembly strategy to selectively form cagelike metallasiloxane molecules with well-defined architectures through the hydrolytic condensation of various organotrialkoxysilanes in the presence of equimolar amounts of alkaline and transition- or lanthanide-metal ions.[6−11] The main forming units in metallasiloxane molecules are one or two stereoregular siloxane cycles fixed on the metal-ion matrix. Reaction of the metallasiloxanes with triorganochlorosilanes or a dilute solution of hydrochloric acid removes the metal ions as metal chlorides and forms the desired stereoregular siloxane cycles.[1−10]

This paper describes the synthesis, characterization, and properties of tris-*cis*-tris-*trans*-dodeca[organo(dimethylorganosiloxy)]cyclododecasiloxanes with the general formula $\{RSiO[OSiMe_2R']\}_{12}$.

EXPERIMENTAL SECTION

Materials. All chemicals used were of high purity and were purchased from Sigma-Aldrich Co. Solvents were dried and distilled

Received: April 20, 2011
Published: September 12, 2011

ACS Publications © 2011 American Chemical Society

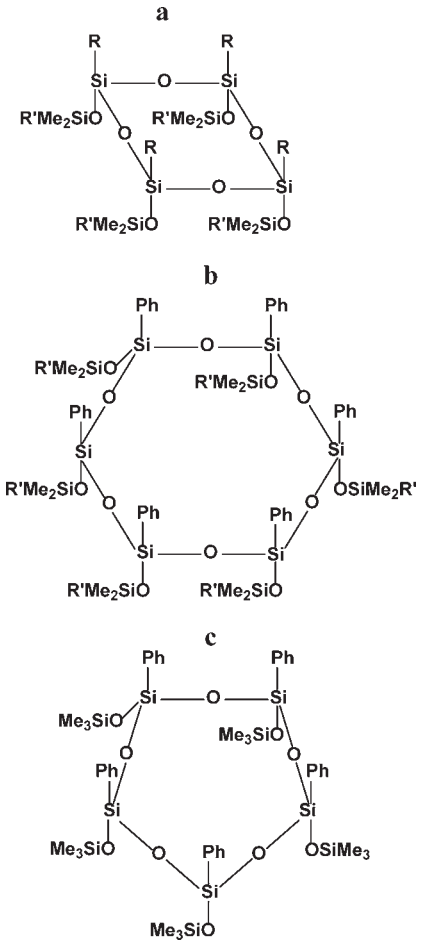

Figure 1. Structural formulas of mesomorphic OCSs.

prior to use.[12] Anhydrous $CuCl_2$ was prepared by heating its crystallohydrate at 120 °C until constant weight.

Characterization Techniques. *NMR Spectroscopy.* ^1H and ^{29}Si NMR spectra were recorded with a Bruker AMX spectrometer (400.1 MHz for ^1H and 79.5 MHz for ^{29}Si) at 20 °C using $CDCl_3$ as a solvent and tetramethylsilane as an internal reference standard.

Differential Scanning Calorimetry (DSC). A DSC study was carried out on a Mettler-822e differential scanning calorimeter at a heating rate of ±10 °C/min under an argon atmosphere. Thermogravimetric analysis (TGA) was performed by Derivatograph-C (MOM, Hungary) on samples with weight of about 20 mg at a heating rate of 5 °C/min in air. The temperature at which a weight loss of 1% was detected was considered to be the decomposition onset temperature.

X-ray Analysis. X-ray analysis was performed with filtered Cu Kα radiation using a DRON-3 M X-ray diffractometer with an asymmetric focusing monochromator (a bent quartz crystal), equipped with a heating and cooling camera, wherein the temperature was automatically regulated. X-ray diffraction (XRD) patterns were measured over a wide temperature range. Phase diagrams were deduced from these XRD patterns. During each experiment, the temperature throughout the sample was controlled with a precision better than 1 °C.

Polarizing Microscopy. The assignments of the transition temperatures were confirmed by polarizing microscopy. Optical birefringence studies were performed on a POLAM-L-213 M polarized microscope with a Linkam LTS350 temperature stage with a CI94 computer interface controller and a LTS-LNP94/2 automated liquid-nitrogen-cooling pump.

Rheological Studies. The flow process was investigated with a MV-2[22] load capillary viscosimeter under a constant shear stress regime. The diameters of the capillaries were 0.7 and 1.6 mm.

Synthesis Procedures. Tris-*cis*-tris-*trans*-dodeca[(phenyl)(trimethylsiloxy)]-cyclododecasiloxane $\{PhSiO[OSiMe_3]\}_{12}$, tris-*cis*-tris-*trans*-dodeca[(phenyl)-(dimethylvinylsiloxy)]cyclododecasiloxane $\{PhSiO[OSiMe_2Vi]\}_{12}$, tris-*cis*-tris-*trans*-dodeca[(phenyl)(dimethylchloromethylsiloxy)]cyclododecasiloxane $\{PhSiO[OSiMe_2CH_2Cl]\}_{12}$, tris-*cis*-tris-*trans*-dodeca[(methyl)-(trimethylsiloxy)]cyclododecasiloxane $\{MeSiO[OSiMe_3]\}_{12}$, and tris-*cis*-tris-*trans*-dodeca[(vinyl)(trimethylsiloxy)]cyclododecasiloxane $\{ViSiO[OSiMe_3]\}_{12}$ were synthesized according to previously described procedures.[6,8−11]

Copper/Sodium Ethylsiloxane. An amount of 2.5 g (0.0626 mol) of NaOH was added to a solution of 10 mL (0.0626 mol) of $EtSi(OMe)_3$ in 80 mL of *n*-butanol under vigorous stirring at room temperature. Then, 3.38 mL (0.1878 mol) of H_2O was added dropwise, and the mixture was stirred for 15 min. The mixture was then heated, and a hot solution of 2.8 g (0.0208 mol) of $CuCl_2$ in 40 mL of *n*-butanol was added dropwise prior to bringing the mixture to boiling for 20 min. The NaCl precipitate was filtered off of the solution. Upon standing at room temperature for 2 days, crystals of copper/sodium ethylsiloxane were formed in the solution. The yield of blue crystals was 4.02 g (54.3%). Anal. Calcd for $\{Na_4[(EtSi(O)O)_{12}Cu_4]\}\cdot 6n$-BuOH ($C_{48}H_{120}Si_{12}Cu_4Na_4O_{30}$): C, 30.98; H, 6.50; Si, 18.12; Cu, 13.66; Na, 4.94. Found: C, 30.57; H, 6.89; Si, 17.77; Cu, 13.14; Na, 4.53.

Tris-*cis*-tris-*trans*-dodeca[(ethyl)(trimethylsiloxy)]cyclododecasiloxane $\{EtSiO[OSiMe_3]\}_{12}$. A mixture of 3.9 g (0.0027 mol) of copper/sodium ethylsiloxane and 7.96 mL (7.82 g, 0.0989 mol) of pyridine was stirred for 10 min at room temperature. Then a solution of 16.69 mL (14.32 g, 0.1318 mol) of Me_3SiCl in 80 mL of hexane was added dropwise. The resulting mixture was refluxed for 1 h. After cooling to room temperature, the reaction mixture was filtered to remove precipitated material and the filtrate was washed with water and dried over Na_2SO_4. The majority of the solvent was evaporated on a rotary evaporator (10 mmHg/40 °C), and the rest was removed under higher vacuum (1 mmHg/90−95 °C, 1 h). A waxlike colorless product was obtained (yield, 3.56 g, 66.5%). Anal. Calcd for $[C_2H_5Si(O)OSi(CH_3)_3]_{12}$ ($C_{60}H_{168}Si_{24}O_{24}$): C, 36.99; H, 8.69; Si, 34.61. Found: C, 37.15; H, 8.93; Si, 34.52. ^1H NMR ($CDCl_3$, δ, ppm): two singlets at 0.12 (9H, *cis*/*cis*-$OSi(CH_3)_3$) and 0.13 (9H, *cis*/*trans*-$OSi(CH_3)_3$) with a ratio of integrated intensities 1:2: 0.52−0.57 (m, 2H, $-O_3SiCH_2CH_3$), 0.97−1.02 (m, 3H, $-O_3SiCH_2CH_3$); a ratio of the integrated intensities of trimethylsiloxy and ethyl groups of protons was 9:5. ^{29}Si NMR ($CDCl_3$, δ, ppm): −68.34 (s, *cis*/*cis*-$OSi(CH_3)_3$), −68.07 (s, *cis*/*trans*-$OSi(CH_3)_3$), 7.08 (s, *cis*/*cis*-$O_3SiC_2H_5$), 7.00 (s, *cis*/*trans*-$O_3SiC_2H_5$).

RESULTS AND DISCUSSION

1. Synthesis of Tris-*cis*-tris-*trans*-dodeca[organo(dimethylorganosiloxy)]cyclododecasiloxanes. The synthesis was carried out in two steps: synthesis of copper(II) organosiloxane, followed by its reaction with triorganochlorosilane (Schemes 1 and 2). Hydrolysis of organotrialkoxysilanes in the presence of an equimolar amount of NaOH or KOH in alcohol media leads to the formation of a labile alkaline intermediate **A** containing ion pairs, which tend to associate, forming complex aggregates **B**. The components of the hydrophilic layer (alkali metal ions, alcohol, and water molecules) of **B** are surrounded by silicon species containing functional OX groups (X = H, R′). After the addition of $CuCl_2$, a partial exchange of Na^+/K^+ ions by Cu^{2+} ions takes place, resulting in the formation of aggregates **C**. The functional groups attached to organosilicon fragments are involved in condensation to form organosiloxanolate rings fixed on a "metallic matrix", i.e.,

Scheme 1. Formation of Copper/M Organosiloxane Molecules

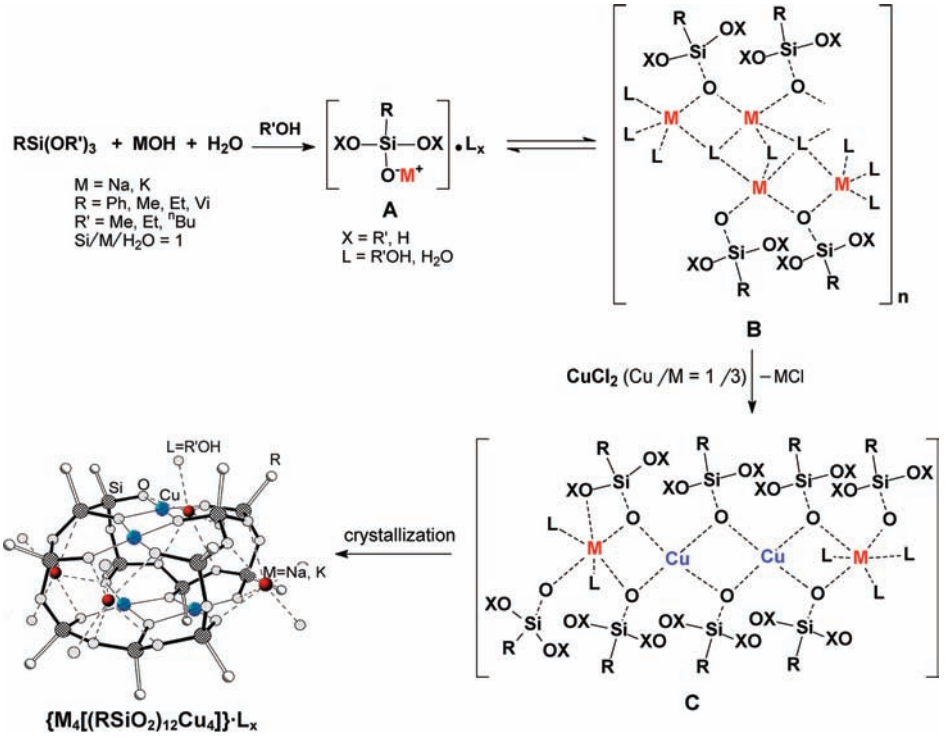

Scheme 2. Synthesis of Dodeca[organo(triorganylsiloxy)]cyclododecasiloxanes

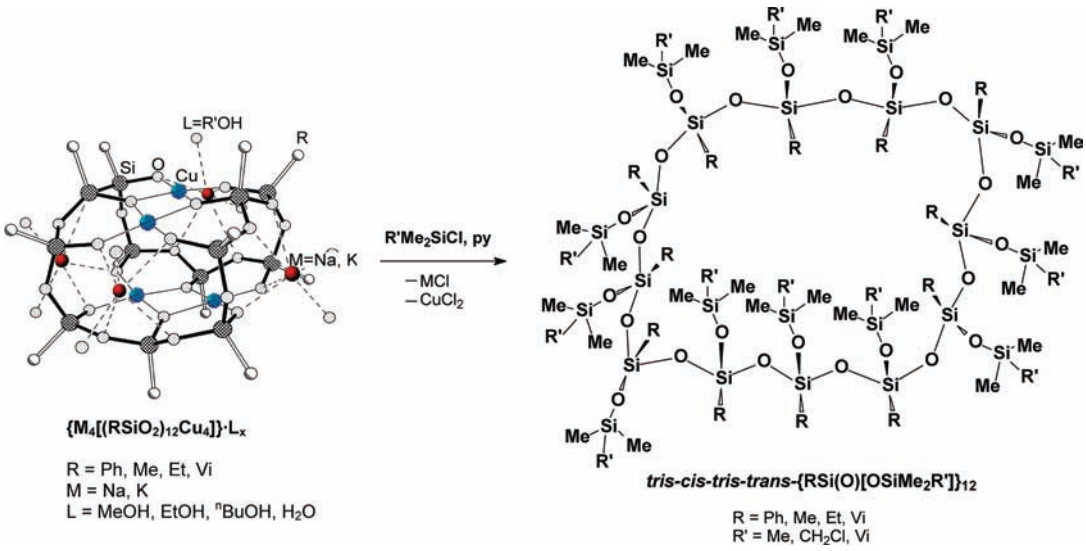

copper/M siloxane molecules $\{M_4[(RSiO_2)_{12}Cu_4]\}\cdot L_x$ (Scheme 1). The basic structural unit of the molecule is a cyclododecasiloxanolate fragment of tris-*cis*-tris-*trans* configuration and a horse-saddle conformation. The subsequent reaction of copper/M siloxane with $Me_2R'SiCl$ (R′ = Me, CH_2Cl, Vi; Scheme 2) results in the formation of the corresponding stereoregular organocyclododecasiloxanes. The presence of substituents of two different types at silicon, R and $OSiMe_2R'$, imparts partially broken "up-and-down" symmetry.

2. Phase Transition Behavior. On the basis of their property differences, the cyclododecasiloxanes $\{RSiO[OSiMe_2R']\}_{12}$ can be divided into two groups. The first group includes $\{RSiO[OSiMe_2R']\}_{12}$ with R = Ph and R′ = Me, CH_2Cl, Vi. These compounds exist in a solid state or mesophase up to their decomposition temperature. The second group, $\{RSiO[OSiMe_2R']\}_{12}$ with R = Me, Vi, Et and R′ = Me, exists in a liquid or mesomorphic state above the glass transition temperature. Cyclododecasiloxanes are presented in Table 1.

dx.doi.org/10.1021/ic2008123 |*Inorg. Chem.* 2011, 50, 10033–10040

Table 1. Designations of Tris-*cis*-tris-*trans*-dodeca[organo-(dimethylorganosiloxy)]cyclododecasiloxanes $\{RSiO[OSiMe_2R']\}_{12}$ and Data of TGA

	R	R′	T_{dec}, °C (in air)
Dodeca[phenyl(dimethylorganosiloxy)]cyclododecasiloxanes $\{PhSiO[OSiMe_2R']\}_{12}$			
$PhSi_{12}$-Me	Ph	Me	350
$PhSi_{12}$-CH_2Cl	Ph	CH_2Cl	315
$PhSi_{12}$-Vi	Ph	Vi	270
Dodeca[organo(trimethylsiloxy)]cyclododecasiloxanes $\{RSiO[OSiMe_3]\}_{12}$			
$MeSi_{12}$-Me	Me	Me	200
$ViSi_{12}$-Me	Vi	Me	200
$EtSi_{12}$-Me	Et	Me	230

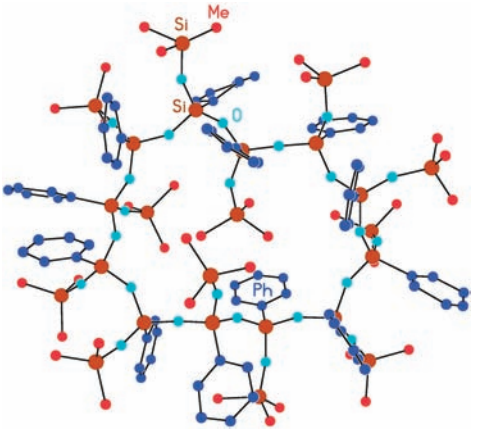

Figure 2. Molecular structure of tris-*cis*-tris-*trans*-dodeca[phenyl-(trimethylsiloxy)]cyclododecasiloxane $PhSi_{12}$-Me with partially broken "up-and-down" symmetry.

2.1. Dodeca[phenyl(dimethylorganosiloxy)]cyclododecasiloxanes $\{PhSiO[OSiMe_2R']\}_{12}$ with R′ = Me, CH_2Cl, Vi. ***2.1.1. $PhSi_{12}$-Me.*** $PhSi_{12}$-Me is a white crystalline compound[10] at room temperature. Its molecular structure (Figure 2) and supramolecular architecture (Figure 3) are determined by the size of the siloxane cycle, flexibility of the siloxane bond, tris-*cis*-tris-*trans* conformation, and "up-and-down" symmetry. DSC shows that upon first heating $PhSi_{12}$-Me undergoes three transitions at 100, 136, and 179 °C (Figure 4, curve 1). Upon second heating, these transitions are not reproduced and the DSC contains only a glass step at $T = -3$ °C (Figure 4, curve 2). According to the TGA data (Table 1 and Figure S1 in the Supporting Information), the decomposition onset temperature of $PhSi_{12}$-Me is 350 °C.

To establish the type of thermotropic transitions observed by DSC, powder XRD patterns were obtained at different temperatures (Figure 5). At room temperature, the initial $PhSi_{12}$-Me sample exhibits the XRD pattern shown in Figure 5, curve 1. Upon heating to 102 °C, the XRD pattern changes, but the presence of a considerable number of Bragg peaks indicates that the crystalline order remains (Figure 5, curve 2). Hence, the compound undergoes a "crystal−crystal" transition at 100 °C.

The XRD pattern obtained at 140 °C (Figure 5, curve 3) differs appreciably from the previous ones: several peaks exist in the region of $2\theta = 3-15°$, and very weak peaks located on a wide amorphous halo in the wide angular region of $2\theta = 15-40°$. Upon further heating above 179 °C, the peaks at $2\theta = 3-15°$ change slightly, the peaks at $2\theta = 15-40°$ disappear, but the wide amorphous halo remains (Figure 5, curve 5). This indicates that $PhSi_{12}$-Me undergoes a two-stage transition to a mesomorphic state in the temperature region of 100−179°. All solid-phase

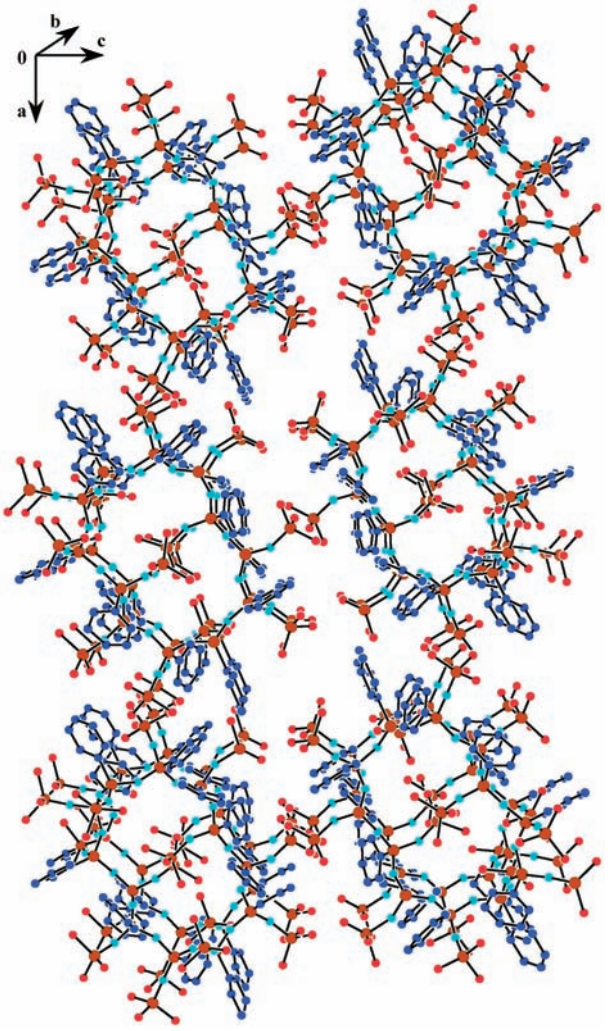

Figure 3. Supramolecular architecture of $PhSi_{12}$-Me.

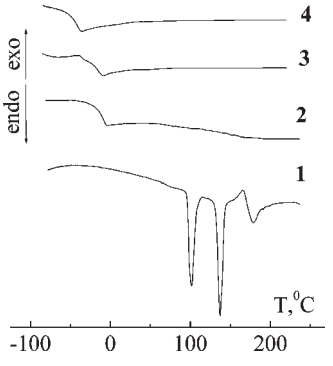

Figure 4. DSC curves obtained upon first heating for the compounds Ph_{12}-Me (1), Ph_{12}-CH_2Cl (3), Ph_{12}-Vi (4) and upon second heating for the compound Ph_{12}-Me (2).

dx.doi.org/10.1021/ic2008123 |*Inorg. Chem.* 2011, 50, 10033–10040

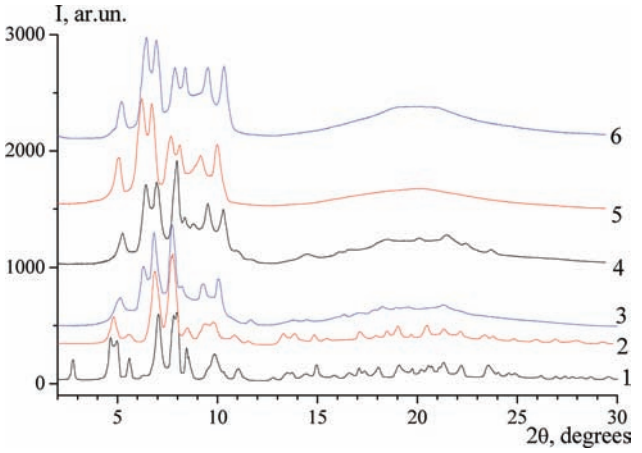

Figure 5. Powder XRD patterns of the compound Ph_{12}-Me at 20 °C (1), 102 °C (2), and 140 °C (3), at 20 °C after cooling from 140 °C (4), at 200 °C (5), and at 20 °C after cooling from 200 °C (6).

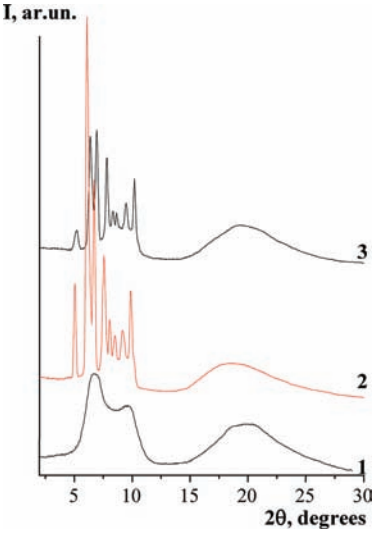

Figure 6. Powder XRD pattern of the native Ph_{12}-CH_2Cl at 20 °C (1) and 207 °C (2) and at 20 °C after cooling from 207 °C (3). Curve 3 is identical with the XRD pattern of Ph_{12}-CH_2Cl crystallized from methanol at 20 °C.

transitions detected upon first heating are irreversible (compare curves 3 with 4 and curves 5 and 6). This fact can be explained by irreversible conformational changes of the macromolecules. Upon cooling from 200 °C to room temperature, the sample remains in a mesomorphic state (Figure 5, curve 6). These data correlate with the DSC trace, which shows only the glass transition at $T_g = -3$ °C (Figure 4, curve 2).

2.1.2. Ph_{12}-CH_2Cl. Ph_{12}-CH_2Cl has a decomposition onset at 315 °C and Ph_{12}-Vi at 270 °C (Table 1 and Figure S1 in the Supporting Information). DSC scans for Ph_{12}-CH_2Cl and Ph_{12}-Vi reveal no thermal effects up to the decomposition temperature (Figure 4). Only stepwise changes of the heat capacity in the glass transition region at −23 °C ($PhSi_{12}$-CH_2Cl) and −43 °C ($PhSi_{12}$-Vi) were observed.

2.1.3. Ph_{12}-CH_2Cl. Ph_{12}-CH_2Cl has been obtained in the amorphous state after synthesis (Figure 6, curve 1). The XRD pattern of this sample corresponds to the superposition of three

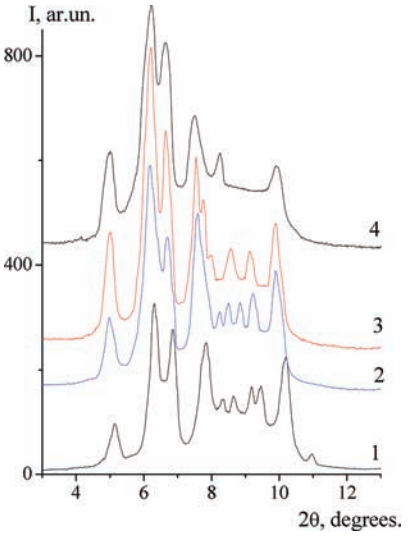

Figure 7. Powder XRD patterns of Ph_{12}-Vi at 20 °C (1), 145 °C (2), 172 °C (3), and 240 °C (4). The angular region of 2θ =15−30° is not presented because an amorphous halo fixed in this region has an appearance identical with those presented in Figures 4 (curves 5 and 6) and 6 (curves 3 and 4).

amorphous halos. Figure 6 shows that, after reaching 190 °C, the pattern changes significantly toward an ordered structure (curve 2). This XRD pattern, which is characteristic of the mesomorphic structure, is maintained unaltered up to 260 °C and down to 20 °C after subsequent cooling (Figure 6, curve 3). The mesomorphic structure of $PhSi_{12}$-CH_2Cl can also be obtained upon recrystallization of an amorphous sample from methanol.

XRD characterization of $PhSi_{12}$-Vi (Figure 7) shows that this compound is in the mesomorphic state regardless of the synthesis and crystallization conditions.

The DSC results are in agreement with the X-ray data. $PhSi_{12}$-CH_2Cl and $PhSi_{12}$-Vi remain mesomorphic in the whole temperature range below their decomposition temperature, forming a mesomorphic glass below T_g. Note that the XRD patterns of all dodeca[phenyl(dimethylorganosiloxy)]cyclododecasiloxanes $PhSi_{12}$-R′ in the mesomorphic state are similar (compare XRD patterns 5 and 6 in Figure 5 with 2 and 3 in Figure 6 and with curves 1−4 in Figure 7), indicating the identity of their mesophase organization.

2.2. Dodeca[organo(trimethylsiloxy)]cyclododecasiloxanes $\{RSiO[OSiMe_3]\}_{12}$ with R = Me, Et, Vi. At room temperature, the compounds $MeSi_{12}$-Me and $ViSi_{12}$-Me are transparent viscous liquids with refraction indexes of 1.4348 and 1.4130, respectively. On the basis of TGA data, these compounds are stable up to 200 °C (Table 1 and Figure S2a in the Supporting Information). DTA reveals exothermic effects in the temperature region of weight loss (Figure S2b in the Supporting Information). The same effect is observed at higher temperature for $MeSi_{12}$-Me than $ViSi_{12}$-Me. This difference is probably due to the higher thermal stability of the methyl groups. It seems that the exothermic effect observed for the compound $ViSi_{12}$-Me in the temperature region of 185−310 °C (Figure S2b, curve 2, in the Supporting Information) is due to the cleavage of vinyl bonds and the formation of intermolecular cross-links that lead to a slowdown of the weight loss.

In contrast to $MeSi_{12}$-Me and $ViSi_{12}$-Me, the compound $EtSi_{12}$-Me is a waxlike material at room temperature. Its decomposition

dx.doi.org/10.1021/ic2008123 |*Inorg. Chem.* 2011, 50, 10033–10040

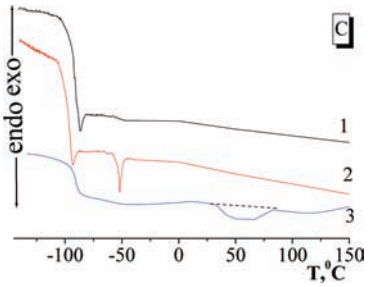

Figure 8. DSC curves for the compounds Me_{12}-Me (1), Vi_{12}-Me (2), and Et_{12}-Me (3) obtained in air (heating speed, 5 °C/min; the sample mass is about 12 mg).

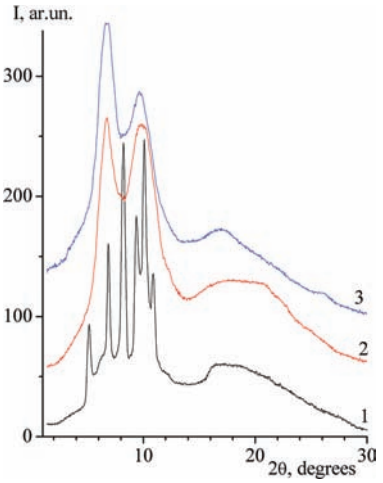

Figure 9. XRD patterns for Et_{12}-Me at 20 (1), 65 (2), and 120 °C (3).

onset temperature is 230 °C (Table 1 and Figure S2a, curve 3, in the Supporting Information).

DSC of the dodeca[organo(trimethylsiloxy)]cyclododecasiloxanes (Figure 8) shows that the compounds with Me and Vi substituents are noncrystallizable: only glass transitions are detected on heating scans at −91 and −97 °C for $MeSi_{12}$-Me and $ViSi_{12}$-Me. Rheological studies of $MeSi_{12}$-Me and $ViSi_{12}$-Me have shown that they are Newtonian liquids. Their flow curves at various temperatures demonstrate the independence of the viscosity value from the shear rate in the range of 20−165 °C (see Figures S3−S5 in the Supporting Information). The wide range of Newtonian flow allows application of the compounds as standard liquids in metrology. Viscous flow energy values calculated from the temperature dependences of viscosity (Figure S4 in the Supporting Information) are 26 and 32 kJ/mol, respectively (Figure S5 in the Supporting Information). These values are greater than that of poly(dimethylsiloxane) (PDMS; 15 kJ/mol).

The DSC of compound $EtSi_{12}$-Me (Figure 8, curve 3) is comprised of a glass transition at −98 °C and a wide slight endothermic peak (1.4 J/g) centered at 55 °C. Taking into account this endo peak and waxylike form of the sample, we propose that compound $EtSi_{12}$-Me is in a mesomorphic state below the transition at 55 °C. The mesomorphic structure of $EtSi_{12}$-Me is confirmed by XRD. Figure 9 shows that this compound is mesomorphic at 20 °C (curve 1) and possesses a reversible transition in the isotropic melt above 55 °C (curves 2 and 3).

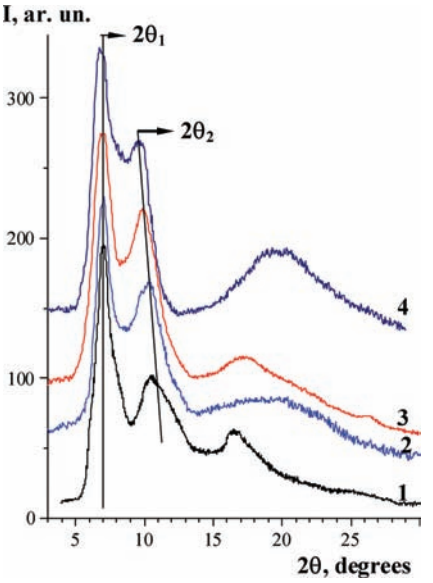

Figure 10. XRD patterns for liquid Me_{12}-Me (1), Vi_{12}-Me (2), and amorphous Ph_{12}-CH_2Cl (4) obtained at 20 °C and for the melt of Et_{12}-Me obtained at 70 °C (3).

The XRD pattern of the $EtSi_{12}$-Me melt is comprised of three amorphous halos (Figures 9, curves 2 and 3, and 10, curve 3). These features are inherent to the XRD patterns of the liquid $MeSi_{12}$-Me and $ViSi_{12}$-Me (Figure 10, curves 1 and 2) and of the amorphous $PhSi_{12}$-CH_2Cl (Figure 10, curve 4). This has not been observed before for any other organosiloxanes. Typically, XRD patterns of well-known linear and cyclic organosiloxanes in the liquid state are comprised of two amorphous halos: the first halo is situated in the angular region of $2\theta^* = 4-14°$ and the second one at $2\theta^{**} = 14-40°$. The typical XRD patterns for four liquid OCSs with different sizes of molecules and for three linear poly(organosiloxanes) with different diameters of macromolecules are cited as an example in Figure 11.

It is known[13] that the intensity distribution for an amorphous scattering $I_a(2\theta)$ in an angular region of $2\theta^*$ is substantially determined by statistics of average intermolecular distances. At the same time, the character of the distribution $I_a(2\theta)$ in the second angular region of $2\theta^{**}$ is generally connected with statistics of average intramolecular distances. Hence, the intensity maximum of the first amorphous halo $2\theta^*_m$ should shift to a smaller angular region (larger intermolecular distances) as the size of the siloxane molecule or the diameter of the poly(organosiloxane) macromolecule increases. This trend is clearly demonstrated in Figure 11, where in the series octamethylcyclotetrasiloxane $[(Me)_2SiO]_4$ (curve 1) → decamethylcyclopentasiloxane $[(Me)_2SiO]_5$ (curve 2) → *cis*-tetrakis[(methyl)(trimethylsiloxy)]cyclotetrasiloxane $[MeSi(O)OSiMe_3]_4$ (curve 3) → tetrakis(trimethylsiloxy)silane $Me_3SiO[SiO(OSiMe_3)_2]SiMe_3$ (curve 4) the value of $2\theta^*_m$ changes as 12.0° → 11.3° → 9.6° → 8.2° and in the series PDMS (curve 5) → poly(diethylsiloxane) (PDES; curve 6) → poly(diphenylsiloxane) (PDPhS; curve 7) as 11.9° → 10.7° → 8.5°.

In contrast to oligo- and poly(organosiloxanes) shown in Figure 11, liquid $MeSi_{12}$-Me and $ViSi_{12}$-Me, the melt of $EtSi_{12}$-Me, and amorphous $PhSi_{12}$-CH_2Cl (Figure 10) are characterized by the presence of two overlapping amorphous halos at $2\theta_1$ and $2\theta_2$ with rather a small half-width of $\Delta_{1/2} = 1.5°$ in the angular

dx.doi.org/10.1021/ic2008123 |*Inorg. Chem.* 2011, 50, 10033–10040

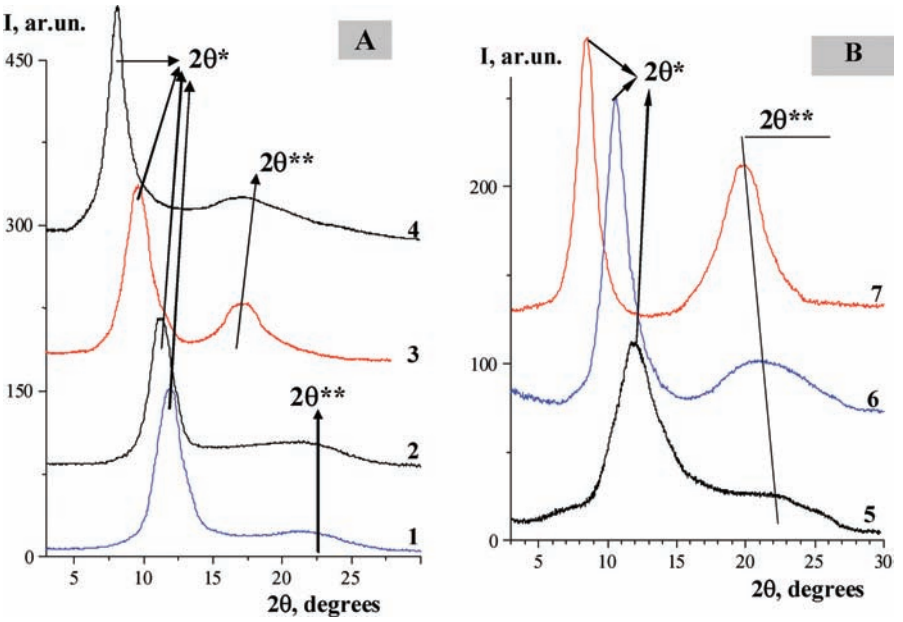

Figure 11. Diffractograms of oligo(organosiloxanes) (A): octamethylcyclotetrasiloxane $[(Me)_2SiO]_4$ (1), decamethylcyclopentasiloxane $[(Me)_2SiO]_5$ (2), *cis*-tetrakis[(methyl)(trimehtylsiloxy)]cyclotetrasiloxane $[MeSi(O)OSiMe_3]_4$ (3), and tetrakis(trimethylsiloxy)silane $(Me_3SiO[SiO(OSiMe_3)_2]$-$SiMe_3$ (4). Poly(organosiloxanes) (B): PDMS (5), PDES (6), and PDPhS (7).

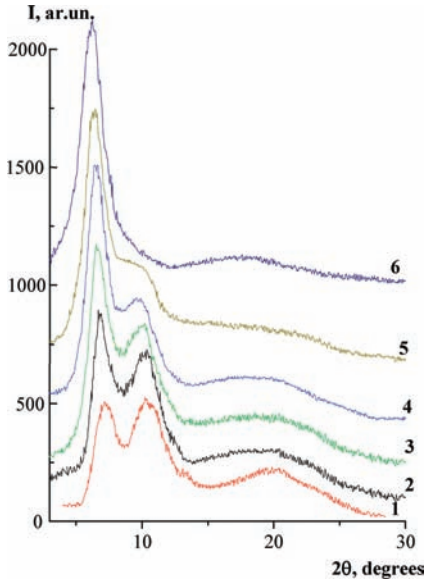

Figure 12. Diffractograms of $ViSi_{12}$-Me obtained at various temperatures: (1) −8 °C; (2) 20 °C; (3) 120 °C; (4) 180 °C; (5) 210 °C; (6) 275 °C.

region of $2\theta^*$. This peculiar feature of amorphous scattering of the macrocycles is associated with the molecular structure of the cycles.

As was mentioned above, the broken "up-and-down" symmetry is differentiating the molecular structures of $MeSi_{12}$-Me, $ViSi_{12}$-Me, $EtSi_{12}$-Me, and $PhSi_{12}$-CH_2Cl. These cycles with high chain flexibility have two different types of substituents: an organic R group and a triorganosiloxy $OSiMe_2R'$ group. For the compounds $MeSi_{12}$-Me, $ViSi_{12}$-Me, and $EtSi_{12}$-Me, the triorganosiloxy side groups are equal (R′ = Me). Compound $PhSi_{12}$-CH_2Cl has a larger triorganosiloxy side group. At the same time, the organic side groups R are different for each compound and smaller than the triorganosiloxy groups $OSiMe_2R'$. The features of the chemical composition of the side groups relate directly to the specific character of their diffraction. Analysis of the XRD patterns in Figure 10 shows that the angular positions of the maxima of the first amorphous halo $2\theta_1$ differ very slightly: $2\theta_1$ = 7.0, 6.9, 6.9, and 6.7° for $MeSi_{12}$-Me, $ViSi_{12}$-Me, $EtSi_{12}$-Me, and $PhSi_{12}$-CH_2Cl, respectively. At the same time, the angular positions of the maxima of the second amorphous halo $2\theta_2$ shift to a smaller angular region as the size of the side group R increases in the series Me → Vi → Et → Ph. The insignificant decrease of the angular position $2\theta_1$ for $PhSi_{12}$-CH_2Cl is quite logical and is associated with the large size of the group $OSiMe_2CH_2Cl$.

The appearance of two amorphous halos ($2\theta_1$ and $2\theta_2$) in the region of $2\theta^* = 4-14°$ is most probably related to the presence of two predominant types of inter- and intramolecular contacts substantially differing in their distance Si···Si, which are Si−R···R−Si and Si−Me_2R'···$R'Me_2$−Si. In other words, for the macrocycles, it is possible to propose the presence of a microphase separation on inter- and intramolecular levels, which is due to the structure and high flexibility of the macrocycles. As a result, the compounds $MeSi_{12}$-Me, $ViSi_{12}$-Me, and $EtSi_{12}$-Me should form labile substructures.

The stability of these substructures was studied through temperature-dependent X-ray diffractometry. Figure 12 shows the XRD patterns of $ViSi_{12}$-Me. In the angular region of $2\theta^*$, the intensity redistribution between $2\theta_1$ and $2\theta_2$ occurs with increasing temperature, and only one maximum is observed in the angular region of $2\theta^*$ at 275 °C. This change is irreversible because a cross-linking process through the vinyl groups occurs at this temperature according to TGA and DTA data (Figure S2 in the Supporting Information).

The X-ray scattering of $MeSi_{12}$-Me at various temperatures showed a similar trend in the redistribution of intensities in the region of $2\theta^*$. However, in this case all changes have reversible character.

dx.doi.org/10.1021/ic2008123 |*Inorg. Chem.* 2011, 50, 10033–10040

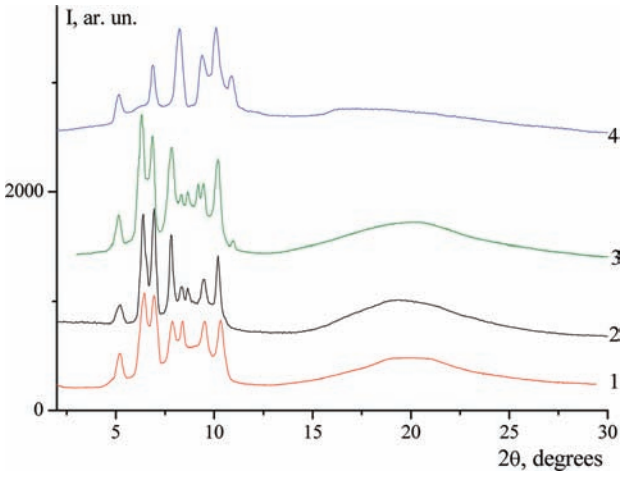

Figure 13. Diffractograms obtained for $PhSi_{12}$-Me (1), $PhSi_{12}$-CH_2Cl (2), $PhSi_{12}$-Vi (3), and $EtSi_{12}$-Me (4) in the mesomorphic state.

When the packing in a crystal is known (as in the case of $PhSi_{12}$-Me; see Figure 3) and the mesophase shows birefringence, it is possible to make a conjecture regarding the molecular packing in the mesophase. Identification of the type of mesomorphic order of the cycles $PhSi_{12}$-Me, $PhSi_{12}$-CH_2Cl, $PhSi_{12}$-Vi, and $EtSi_{12}$-Me is difficult. The fact that the set of reflexes of the mesophase of compounds $PhSi_{12}$-Me, $PhSi_{12}$-CH_2Cl, and $PhSi_{12}$-Vi (Figure 13, curves 1−3) does not vary with a change of the side groups is of interest. Comparison of the diffractograms of $PhSi_{12}$-Me and $EtSi_{12}$-Me (Figure 13, curves 1 and 4) is especially surprising because the volume of the $EtSi_{12}$-Me molecule is essentially less. On the basis of the data obtained, we believe that the molecular packing of the cycles in the mesophase is columnar or noncubic of odis type.

CONCLUSION

Cyclic organosiloxanes with the general formula $\{RSiO[OSiMe_2R']\}_{12}$ show a strong tendency to self-organize in ordered noncrystalline structures. The type of substituents R and R′ is the major factor influencing the processes of self-organization of these cyclosiloxanes in ordered structures and determining their mesomorphic properties.

Macrocyclic OCSs with phenyl organic substituents (R = Ph) form mesomorphic structures within a very wide temperature range. The organododecasiloxanes with aliphatic substituents RSi_{12}-Me (R = Me, Vi, Et and R′ = Me) tend to microphase-separate on intra- and intermolecular levels in a liquid state, forming labile substructures.

Upon an increase in the length of the organic substituent, i.e., when R = Et, an interaction between the ethyl groups appears sufficient for the formation of mesomorphic structures, within a relative narrower range than that in compounds with R = Ph.

It is important to point out that, for the cyclododecasiloxanes under consideration, for the cyclotetrasiloxanes $\{RSiO[OSiMe_3]\}_4$, which were investigated earlier,[1,4] and for the known linear mesomorphic poly(organosiloxanes)[14−17] $[-OSi(R_2)-]_n$, variation of the type of substituent R leads to identical changes of the mesomorphic properties in spite of the fact that the type of mesomorphic ordering for these three groups of compounds is different.

ASSOCIATED CONTENT

Supporting Information. TGA, DTA, and flow curves, temperature dependence of the viscosity values, and viscous flow energy values. This material is available free of charge via the Internet at http://pubs.acs.org.

AUTHOR INFORMATION

Corresponding Author
*E-mail: olga@ineos.ac.ru.

REFERENCES

(1) Matukhina, E. V.; Shchegolikhina, O. I.; Makarova, N. N.; Pozdniakova, Yu. A.; Katsoulis, D.; Godovskiy, Yu. K. *Liq. Cryst.* **2001**, *28*, 869.
(2) Matukhina, E. V.; Shchegolikhina, O. I.; Molodtsova, Yu. A.; Pozdniakova, Yu. A.; Lyssenko, K. A.; Vasil'ev, V. G.; Buzin, M. I.; Katsoulis, D. E. *Liq. Cryst.* **2004**, *31*, 401.
(3) Pozdniakova, Yu. A.; Chetverikov, A. A.; Lyssenko, K. A.; Peregudov, A. S.; Buzin, M. I.; Matukhina, E. V.; Shchegolikhina, O. I. *Russ. Chem. Bull.* **2007**, *56*, 77.
(4) Shchegolikhina, O. I.; Pozdniakova, Yu. A.; Chetverikov, A. A.; Peregudov, A. S.; Buzin, M. I.; Matukhina, E. V. *Russ. Chem. Bull.* **2007**, *56*, 83.
(5) Molodtsova, Yu. A.; Shchegolikhina, O. I.; Peregudov, A. S.; Buzin, M. I.; Matukhina, E. V. *Russ. Chem. Bull.* **2007**, *56*, 1402.
(6) Molodtsova, Yu. A.; Pozdniakova, Yu. A.; Lyssenko, K. A.; Blagodatskikh, I. V.; Katsoulis, D. E.; Shchegolikhina, O. I. *J. Organomet. Chem.* **1998**, *571*, 31.
(7) Pozdniakova, Yu. A.; Lyssenko, K. A.; Korlyukov, A. A.; Blagodatskikh, I. V.; Auner, N.; Katsoulis, D.; Shchegolikhina, O. I. *Eur. J. Inorg. Chem.* **2004**, 1253.
(8) Molodtsova, Yu. A.; Pozdnyakova, Yu. A.; Blagodatskikh, I. V.; Peregudov, A. S.; Shchegolikhina, O. I. *Russ. Chem. Bull.* **2003**, *52*, 2722.
(9) Molodtsova, Yu. A.; Lyssenko, K. A.; Blagodatskikh, I. V.; Matukhina, E. V.; Peregudov, A. S.; Buzin, M. Y.; Vasil'ev, V. G.; Katsoulis, D. E.; Shchegolikhina, O. I. *J. Organomet. Chem.* **2008**, *693*, 1797.
(10) Igonin, V. A.; Molodtsova, Yu. A.; Pozdniakova, Yu. A.; Zhdanov, A. A.; Strelkova, T. V.; Lindeman, S. V. *J. Organomet. Chem.* **1998**, *562*, 141.
(11) Shchegolikhina, O. I.; Pozdnyakova, Yu. A.; Molodtsova, Yu. A.; Korkin, S. D.; Bukalov, S. S.; Leites, L. A.; Lyssenko, K. A.; Peregudov, A. S.; Auner, N.; Katsoulis, D. E. *Inorg. Chem.* **2002**, *41*, 6892.
(12) Gordon, A. J.; Ford, R. A. *The Chemist's Companion*; Wiley-Interscience: New York, 1972.
(13) Skryshevsky, A. F. *Structural analysis of liquids and amorphous solids*; Vysshaya shkola: Moscow, 1980.
(14) Godovsky, Yu. K.; Papkov, V. S. *Adv. Polym. Sci.* **1988**, *88*, 129.
(15) Godovsky, Yu. K.; Papkov, V. S. *Makromol. Chem., Makromol. Symp.* **1986**, *4*, 71.
(16) Godovsky, Yu. K.; Papkov, V. S. *Adv. Polym. Sci.* **1989**, *88*, 129.
(17) Molenberg, A.; Moeller, M.; Sautter, E. *Prog. Polym. Sci.* **1997**, *22*, 1133.